

# Soft Inflatable Fingers: An Overview of Design, Prototyping and Sensorisation for Various Applications

Faisal Aljaber<sup>1\*</sup>, Ahmed Hassan<sup>1\*</sup>, Taqi Abrar<sup>1\*</sup>, Ivan Vitanov<sup>1</sup> and Kaspar Althoefer<sup>1</sup>

**Abstract**—Fabric-based soft actuators, grippers and manipulators are gaining in popularity due to their ability to handle large payloads while being lightweight, extremely compliant, low-cost and fully collapsible. Achieving full-pose sensing of fabric fingers without compromising on these advantageous properties, however, remains a challenge. This paper overviews work on soft fabric-based inflatable finger design, actuation and sensorisation carried out at the Centre for Advanced Robotics at Queen Mary (ARQ), University of London. Further experimental analysis has been performed to examine features such as bending control and eversion (growing from the tip) in fabric fingers for grasping applications. In addition, two types of grasp force have been measured for a bi-fingered gripper: envelope grasping and pinch grasping. Beyond force measurement, this paper advances a new concept for the sensorisation of fabric grippers using soft optical waveguide sensors and proposes shape estimation using image processing.

## I. INTRODUCTION

Grasping and pick-and-place operations are fundamental to manual dexterity in humans and essential to performing many useful tasks that involve object handling. The efficacy of human hand movement in grasping and manipulating objects is remarkable even under external disturbances or stress. Researchers have therefore attempted to design grasping mechanisms close in functionality and efficiency to the human hand. Traditionally, robot gripping systems were designed using rigid components and were often extremely bulky. With increased functionality, which translates to increased degrees of freedom, such systems have grown increasingly complex to assemble and control. Soft robotic grippers are designed from materials that offer inherent compliance and controllable stiffness. A key advantage is that they can be underactuated, offering more degrees of freedom with fewer actuators – much like a human hand where each finger consists of one tendon and three links having only 2 degrees of freedom [1].

A further advantage to using soft materials for robotic gripping is that such materials create less shock upon impact with an object, potentially mitigating gripper-induced damage. Indeed, even in traditional rigid-bodied devices, gripping surfaces tend to be made out of soft materials to minimise impact damage. Another advantage of being underactuated is that soft robotic grippers oftentimes require simpler control

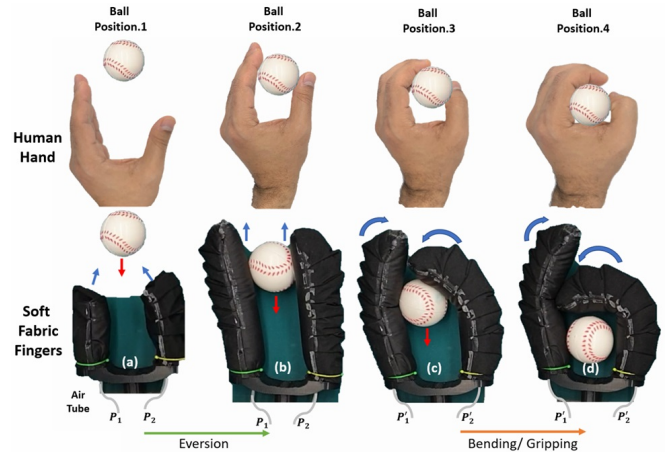


Fig. 1. Fabric-based bi-fingered gripper, exhibiting eversion and bending to reach and grasp an object.

mechanisms during operation, making them easier to design and fabricate.

Soft robots are growing in prominence on account of their inherent safety, compliance, low cost and less complex control needed to operate them [2], [3]. Amongst soft robots, fabric-based devices are of particular interest due to a number of unique attributes, including being lightweight and collapsible. Fabric-based actuators being very low-cost can be manufactured in bulk utilising industrial or programmable sewing machines to generate complex shapes [4]. Due to these attributes, a variety of soft robotic applications have been developed using fabric-based structures to achieve high-payload capability manipulators [5], [6], soft grippers [7] and rehabilitation gloves [8], [9]. Developing soft sensors to enable proprioception of fabric actuators without compromising on these inherent benefits, however, remains a significant challenge.

Fabric-based robot arms and fingers are typically elongated cylindrical structures with folds and pleated structures integrated to achieve bending. Cappello et al. showed how different layering arrangements of fabrics in a pleated geometry can give rise to a range of multi-degree-of-freedom actuators that can operate at low pressures, have a high torque-to-weight ratio and be fully collapsible [8]. A fully fabric-based robotic arm was developed by Liang et al. [5]. Similarly, a wearable robotic arm completely constructed using fabric was also developed [6]. Another novel approach is the fabrication of modular units called fabric-based rotary actuators (FRAs), which — [10]. FRAs are small in size and lightweight. Multiple FRAs can be joined together to form a gripper capable of handling objects much bigger than

\* Equally contributing authors

<sup>1</sup>The authors are with the Centre for Advanced Robotics @ Queen Mary (ARQ), Faculty of Science and Engineering, Queen Mary University of London, Mile End Road, London E1 4NS, U.K. f.aljaber@qmul.ac.uk, ahmed.hassan@qmul.ac.uk; t.abrar@qmul.ac.uk; iv\_vitanov@yahoo.co.uk; k.althoefer@qmul.ac.uk

a single module.

Although fabric actuators offer interesting attributes, they pose major challenges concerning sensorisation and proprioception. Firstly, the outer regions often have features such as pleats or folds which are not ideal for integrating sensor elements. Secondly, fabrics are more pliable than silicone actuators and hence exhibit high local curvature, which can be difficult to measure using integrated sensors. One practical solution is to embed pure bending sensors along the inextensible fabric layer. Elgeneidy et al. embedded commercially available flex sensors into the strain-limiting layer of a soft pneumatic finger to characterise bending [11].

Recent studies have shown that stretchable optical waveguides made of a pair of transparent elastomeric materials can be used to sense longitudinal elongation and bending. Zhao et al. developed stretchable waveguides and integrated them into a soft pneumatic hand to sense bending and normal forces applied to the hand [12]. Teeple et al. used similar sensors in a pneumatic gripper and showed that they are robust in relation to environmental conditions and can be used in deep sea grasping and manipulation [13]. Stretchable waveguides and optical deflections in an optoelectronic foam have also been used to detect changes in the shape of a soft body as a result of bending or twisting, as well as its direction [14], [15].

In all these studies, optical waveguides have been run along the length of the soft bodies and have not addressed local deformations in these bodies. Many studies found in the literature and utilising different sensing technologies tend to also assume constant curvature in soft actuators in order to localise their state via strain or flex sensors [16]. Optics-based sensors to measure displacement as well as force have proven to be very successful [17]. However, as the softness of the body increases, it becomes more prone to exhibiting non-homogeneous deformations. Fabric-based soft actuators in particular comply well to the shape of an object, leading them to assume shapes that are non-homogeneous.

## II. SOFT FABRIC ACTUATOR

Using fabric as the material from which to construct soft fingers has many advantages, including ease and low cost of fabrication, and the need for less sophisticated control due to underactuation and compliance. In comparison to fluidic elastomer actuators, one of the most popular materials used in the construction of soft fingers, fabric actuators do not require complicated material preparation and moulds in their fabrication.

In this paper, we present three separate finger designs, capable of performing different operations: 1) **fabric-based bending finger**: a finger capable of performing a bending operation when actuated; 2) **fabric-based eversion finger**: a finger performing an eversion (growing from tip) operation when actuated; and 3) **fabric finger capable of both bending and eversion**: the final design incorporates both the bending and eversion capabilities of the previous two designs.

### A. Fabric-based bending finger

For grasping applications, we need an actuator to perform controlled bending. A finger made of soft, inextensible fabric has to have some extra material on one side in order to facilitate the bending motion upon actuation. This extra material should be opposite to the bending direction of the finger. The extra material is introduced in the finger in the form of folds or pleats sewn into the structure of the finger. This design is of a very basic construction. It was used to test and evaluate the construction of pleats and their effectiveness in bending a fabric actuator. The fabric finger gets very stiff when pressurised but does not bend under normal construction (construction without any pleats on any side); the fabric finger can achieve a bend of more than 180 degrees upon pressurisation if enough material is introduced to aid the bending in the form of pleats. This type of bending is shown in Figure 2.

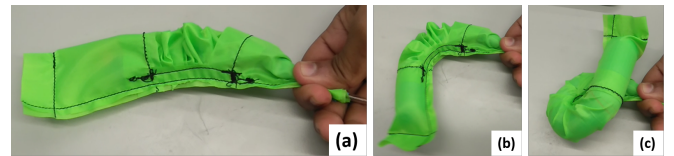


Fig. 2. Fabric finger bending at different angles after the introduction of pleats: (a) initial state; (b) achieving a 90° bend; and (c) fully bent at around 270°.

The actuation is performed by applying air pressure into the fabric finger. Fingers are constructed by stitching the layers together, which introduces pinpricks in the fabric, causing air leakage. To avoid air leakage, an extra layer of plastic is placed inside the bending chamber to contain the air inside and maximise the effect of actuation as shown in Figure 4(a).

### B. Fabric-based eversion finger

Eversion is a concept which is inspired by the growth of vines [18]. By applying this principle to a fabric-based finger, it can be made to extend in length during actuation. To implement this idea, the upper part of the finger, which is cylindrical in shape, is folded inwardly into the structure. The design enables the finger to "evert" or grow from the tip from a folded state to a fully extended state when pneumatic pressure is applied, as shown in Figure 1. This capability is particularly useful in hard to reach environments – see [18]. These robots can be used for applications like remote photography, the deployment of mobile and portable antennas [19], and in human surgery, where the surrounding area is very sensitive and the space narrow and tight – examples being endoscopy or colonoscopy [20].

Other uses of eversion robots include fabric-based structures [21]–[24] with high payload and force generation capabilities. Given their strength and ease of access, these fabric-based structures ensure high levels of safety when operated in human-robot interaction (HRI) scenarios. The concept of eversion is shown in Figure 3.



Fig. 3. Fabric-based eversion finger growing from the tip when inflated: (a) initial state of the fabric-based eversion finger when no input is given and the finger is in a folded state; (b-d) pressure input causes the finger to start growing from the tip by turning out its folds; (e) the finger is fully everted and achieves its maximum length [23].

As with the fabric-based bending finger, the eversion finger has an air leakage issue because of the stitch holes; however, ameliorating this by using a plastic lining within the fabric layer would increase the overall weight of the structure, hindering the eversion process. Instead, we used adhesive iron-on fabric tape before stitching the layers together, as shown in Figure 4(b). The tape prevents most of the air escaping from the finger structure and keeps the overall weight light enough that it can perform the eversion operation efficiently.

### C. Fabric finger capable of both bending and eversion

Having fabricated fingers able to bend, and others able to evert, we developed a new design which incorporated both bending and eversion capability for a single structure. The new design consists of three fabric layers, one with pleats and two plain fabric layers. By stitching together the three fabric layers, we create two chambers. Based on their respective uses, these are referred to as the bending chamber and the eversion chamber. The detailed structure of the hybrid finger design is shown in Figure 4(c).

As previously mentioned, applying actuation pressure in the eversion chamber causes the finger to unfold and grow from the tip until it reaches its maximum length. Similarly, the actuation pressure in the bending chamber allows the finger to bend away from the side on which the pleats are located. This operation is particularly useful when we wish to grasp an object in a cluttered environment. The finger, initially folded, will evert around the object. After reaching its full length, the finger bends and forms a grip around the desired object. This operation is demonstrated in Figure 1, where the fingers of a soft gripper evert to access the ball and then bend, forming a secure grip. To release the grip, the eversion chamber is actuated again, counteracting the bend in the fingers, which then straighten, releasing the ball.

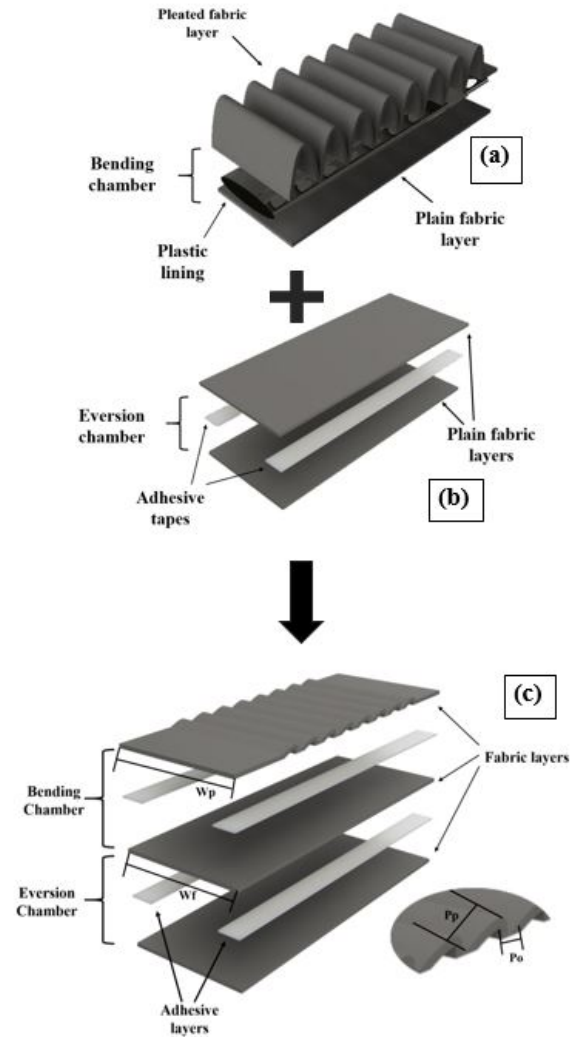


Fig. 4. Exploded views of different fabric finger designs: (a) fabric finger capable of bending, showing one pleated layer and one plain layer combined to form a bending chamber lined with plastic layer; (b) fabric finger with eversion capability, two plain layers sewn together to form an eversion chamber, which unfolds when pressurised – the plastic lining is replaced with adhesive tape to reduce the weight of the finger; and (c) final design, a combination of both bending and eversion chambers, made air-tight using adhesive tape.

## III. SENSING METHODOLOGY

### A. Experimental protocol and setup

In order to capture the non-linear bending behaviour of fabric-based inflatable fingers, we placed three stretchable optical waveguides along the length of a fabric finger, each waveguide providing bending information in a specific region of the finger. The two ends of each optical waveguide are connected via optical fibres to the transmitter and receiver terminals, respectively, of a Keyence FS-N11MN optical fibre amplifier.

The output voltage from the amplifier corresponds to the intensity of light received by the amplifier after passing through the waveguide. In total, we have three output voltage signals (from the three waveguides integrated with the inflatable finger) registering the change in bending in three

areas of the finger. We name the acquired voltage signals "tip"(coloured blue), "middle" (coloured red) and "base" (coloured green), corresponding to the waveguide positions. The placement of the waveguides in the fabric structure is shown in Figure 5.

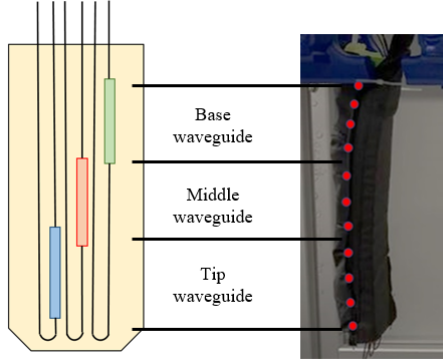


Fig. 5. Details of marker positions corresponding to the three optical waveguides.

### B. Signal loss due to compressive strain on waveguide

A single waveguide, i.e. the sensing element in soft optical-based sensors, is usually subject to several intensity loss mechanisms that may interfere with light transmission. For a transmission disturbance in a waveguide, the signal loss can be modelled in terms of the change in voltage of acquired signals. It is assumed that the voltage signal loss is directly proportional to the intensity loss expressed as a function of deformation, hence the relationship is defined by voltage loss  $V_{loss}$  in decibels as:

$$V_{loss} = 20 \log_{10} \frac{V_{out}}{V_{in}} (dB_v) \quad (1)$$

where  $V_{out}$  is the measured voltage and  $V_{in}$  is the reference voltage when under no deformation.

Figure 6 shows the compression test performed on the sensor used to detect the bending of the fabric finger, and Figure 6(c) shows a logarithmic curve that expresses the relationship between signal loss and compression as it increases.

### C. Image processing pipeline for curve estimation

In our study, the fabric finger was pressurised at 13 different levels of gradation, leading to a planar bending behaviour response. It was observed that the higher the pressure, the greater the bending. For each pressure level, an image of the fabric finger was taken. Each captured image was then processed to extract 11 marker positions placed along the length of the finger and reconstruct the curvature of the fabric finger.

Image processing is performed using the Image Processing Toolbox in MATLAB. During this process, the red markers in the images shown in 7(a) are identified as shown in Figure 7(c), allowing the x-y positions of the marker locations to be

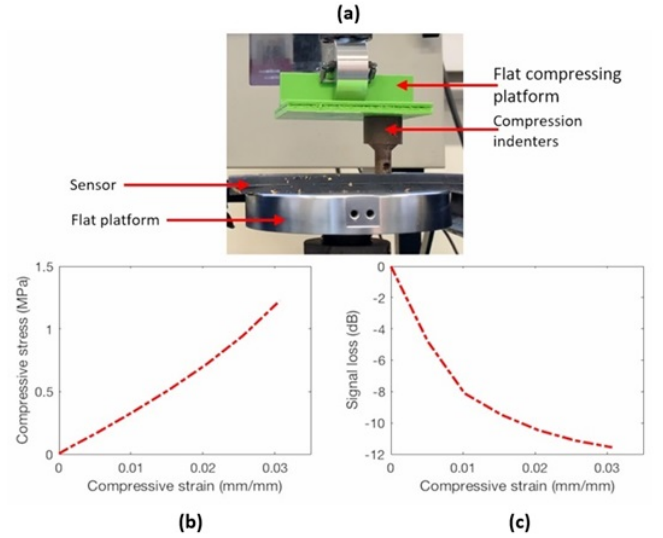


Fig. 6. (a) Experimental setup for applying mechanical compression on a single optical waveguide using a Universal Testing Machine; (b) mechanical stress-strain plot of the waveguide; and (c) logarithmic curve that expresses the relationship between the signal loss and the compression as it increases.

obtained. To achieve this, the binary version of each original image is subtracted from the red segment image to isolate the markers from the rest of the objects in the image. The finger's bending in its plane of operation is visualised by connecting the centre coordinates of the markers. Superimposing the newly created curvature on the original image shows that the curvature detection using markers is successful. The process is shown in Figure 7.

## IV. RESULTS AND DISCUSSION

### A. Optical waveguide sensor results

The fabric finger is actuated to a variety of different pressure values starting at 0 kPa and then increasing to a maximum pressure value of 27.3 kPa before returning back to 0 kPa. The pressure was kept constant for 10 seconds after each pressure change to allow for the motion of the fabric finger to stabilise. The finger's curvature is measured by the three waveguides in three separate regions, each with an integrated waveguide sensor. The results are shown in Figure 8.

From the plot in Figure 8, we observe the following behaviours:

- 1) The middle region (red line) of the fabric finger bent the most under the influence of the input pressure. The base region (green line), which was closest to the fixing assembly, showed no change at all. The fingertip region (blue line) was unaffected at the start but recorded some bending at higher pressure values.
- 2) The middle region of the fabric finger was bent at higher pressures and returned to the original position when the input pressure was reduced back to zero.
- 3) The middle region was very responsive at the start and continued to bend as the pressure increased. However, this region did not return to its original position when the input pressure was reduced back to zero.

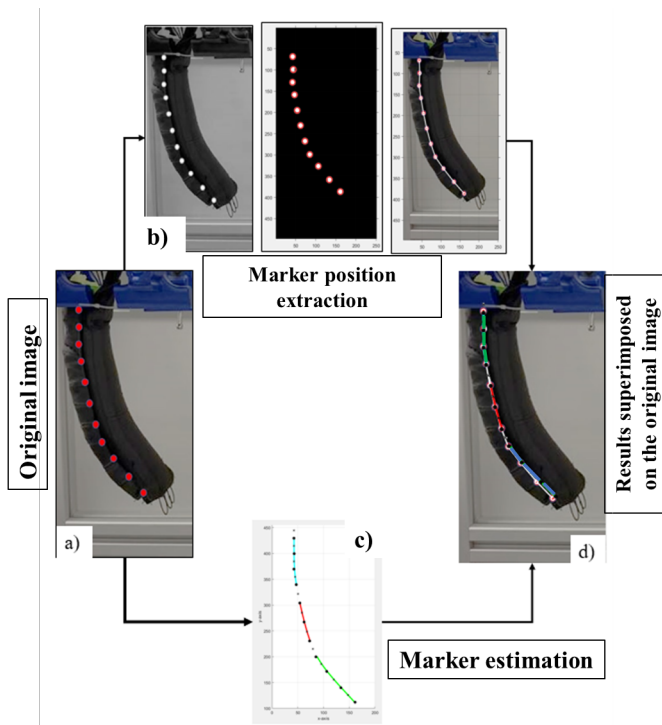


Fig. 7. Fabric finger curvature detection using two separate techniques: (a) original image; (b) marker position extraction by image processing and tracing the positions of the markers on the original image; (c) marker estimation using piece-wise non-linear curve fitting; and (d) results of both techniques superimposed simultaneously on the original image. The path traced after image processing fits well with the marker positions, so it can be used as a reference or ground truth.

### B. Curvature estimation results

To compute the bending behaviour in different regions of the fabric finger using the image processing approach, the x-y locations of the eleven markers along the length of the fabric finger were extracted and further processed. The distribution of the markers, in relation to the optical waveguides, is shown in Figure 5.

As seen in Figure 9, we have superimposed the piece-wise curve fitting plot onto our ground truth model both under zero pressure and maximum pressure conditions.

It was noted that the piece-wise model fits well with the ground truth under zero pressure conditions, but deviates slightly from ground truth under maximum pressure conditions – a consequence, we believe, of non-linear effects. The maximum error is found to be 3.125% for the deviation between the bottom-most ground truth marker and its corresponding location as estimated by the tip waveguide.

## V. CONCLUSIONS

In this paper, we presented different designs of soft fabric-based fingers for robotic gripping applications. We investigated different design methodologies to integrate important features like bending and eversion and were able to develop a design which integrates both of these features efficiently. Combining bending and eversion capabilities enables the gripper to operate in a cluttered environment much more efficiently than a conventional soft gripper. The eversion-

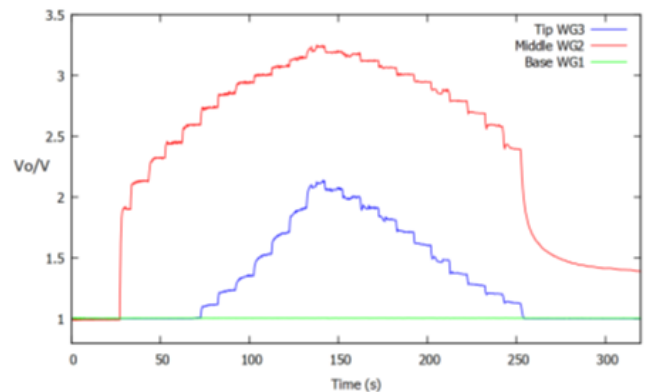


Fig. 8. Output voltage versus time plot for the real-time bending behaviour of the soft fabric-based finger. The bending was achieved by applying increasing values of input air pressure, from 0 kPa to a maximum pressure value of 27.3 kPa and then back to 0 kPa.

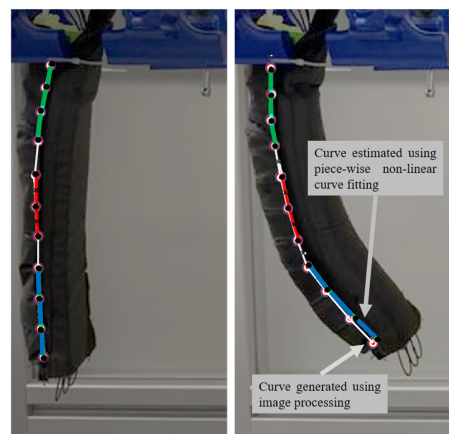


Fig. 9. Combined results of image processing and curve fitting on the original image under 0 and maximum pressure conditions. Note that the curve fitting result deviates slightly from the ground truth towards the bottom.

enabled fingers allow to approach and grip an object which would otherwise be hard to reach.

We also discussed two different approaches to measure the bending behaviour in soft fabric-based fingers. One approach is to integrate soft optical waveguides into three different regions (top, middle and bottom) of the finger. The waveguides record the extent of bending in each particular region independently of each other, enabling us to track local changes in curvature. For benchmarking purposes, we used an alternative vision-based approach.

Marker points overlaid onto the centre line of the fabric-based finger are extracted using image processing and used to reconstruct the finger's shape in the plane. Upon reconstruction, we see that the piece-wise reconstructed model based on our waveguide sensor is capable of estimating the overall finger shape well. To wit, it showed only a small maximum error of about 3% at the fingertip.

## REFERENCES

- [1] J. Shintake, V. Cacucciolo, D. Floreano, and H. Shea, "Soft robotic grippers," *Advanced Materials*, vol. 30, no. 29, p. 1707035, 2018.
- [2] D. Rus and M. T. Tolley, "Design, fabrication and control of soft robots," *Nature*, vol. 521, no. 7553, pp. 467–475, 2015.

- [3] M. Cianchetti, T. Ranzani, G. Gerboni, T. Nanayakkara, K. Althoefer, P. Dasgupta, and A. Menciassi, "Soft robotics technologies to address shortcomings in today's minimally invasive surgery: The stiff-flop approach," *Soft Robotics*, vol. 1, no. 2, pp. 122–131, 2014.
- [4] L. Cappello, K. C. Galloway, S. Sanan, D. A. Wagner, R. Granberry, S. Engelhardt, F. L. Haufe, J. D. Peisner, and C. J. Walsh, "Exploiting textile mechanical anisotropy for fabric-based pneumatic actuators," *Soft robotics*, vol. 5, no. 5, pp. 662–674, 2018.
- [5] X. Liang, H. Cheong, Y. Sun, J. Guo, C. K. Chui, and C.-H. Yeow, "Design, characterization, and implementation of a two-dof fabric-based soft robotic arm," *IEEE Robotics and Automation Letters*, vol. 3, no. 3, pp. 2702–2709, 2018.
- [6] X. Liang, H. Cheong, C. K. Chui, and C.-H. Yeow, "A fabric-based wearable soft robotic limb," *Journal of Mechanisms and Robotics*, vol. 11, no. 3, p. 031003, 2019.
- [7] A. Hassan, H. Godaba, and K. Althoefer, "Design analysis of a fabric based lightweight robotic gripper," in *Annual Conference Towards Autonomous Robotic Systems*. Springer, 2019, pp. 16–27.
- [8] L. Cappello, J. T. Meyer, K. C. Galloway, J. D. Peisner, R. Granberry, D. A. Wagner, S. Engelhardt, S. Paganoni, and C. J. Walsh, "Assisting hand function after spinal cord injury with a fabric-based soft robotic glove," *Journal of neuroengineering and rehabilitation*, vol. 15, no. 1, pp. 1–10, 2018.
- [9] H. K. Yap, P. M. Khin, T. H. Koh, Y. Sun, X. Liang, J. H. Lim, and C.-H. Yeow, "A fully fabric-based bidirectional soft robotic glove for assistance and rehabilitation of hand impaired patients," *IEEE Robotics and Automation Letters*, vol. 2, no. 3, pp. 1383–1390, 2017.
- [10] P. M. Khin, H. K. Yap, M. H. Ang, and C.-H. Yeow, "Fabric-based actuator modules for building soft pneumatic structures with high payload-to-weight ratio," in *2017 IEEE/RSJ International Conference on Intelligent Robots and Systems (IROS)*. IEEE, 2017, pp. 2744–2750.
- [11] K. Elgeneidy, N. Lohse, and M. Jackson, "Bending angle prediction and control of soft pneumatic actuators with embedded flex sensors—a data-driven approach," *Mechatronics*, vol. 50, pp. 234–247, 2018.
- [12] H. Zhao, K. O'Brien, S. Li, and R. F. Shepherd, "Optoelectronically innervated soft prosthetic hand via stretchable optical waveguides," *Science robotics*, vol. 1, no. 1, p. eaai7529, 2016.
- [13] C. B. Teeple, K. P. Becker, and R. J. Wood, "Soft curvature and contact force sensors for deep-sea grasping via soft optical waveguides," in *2018 IEEE/RSJ International Conference on Intelligent Robots and Systems (IROS)*. IEEE, 2018, pp. 1621–1627.
- [14] I. Van Meerbeek, C. De Sa, and R. Shepherd, "Soft optoelectronic sensory foams with proprioception," *Science Robotics*, vol. 3, no. 24, 2018.
- [15] H. Xie, H. Liu, S. Luo, L. D. Seneviratne, and K. Althoefer, "Fiber optics tactile array probe for tissue palpation during minimally invasive surgery," in *2013 IEEE/RSJ International Conference on Intelligent Robots and Systems*. IEEE, 2013, pp. 2539–2544.
- [16] T. C. Searle, K. Althoefer, L. Seneviratne, and H. Liu, "An optical curvature sensor for flexible manipulators," in *2013 IEEE International Conference on Robotics and Automation*. IEEE, 2013, pp. 4415–4420.
- [17] H. Xie, A. Jiang, H. A. Wurdemann, H. Liu, L. D. Seneviratne, and K. Althoefer, "Magnetic resonance-compatible tactile force sensor using fiber optics and vision sensor," *IEEE Sensors Journal*, vol. 14, no. 3, pp. 829–838, 2014.
- [18] E. W. Hawkes, L. H. Blumenschein, J. D. Greer, and A. M. Okamura, "A soft robot that navigates its environment through growth," *Science Robotics*, vol. 2, no. 8, 2017.
- [19] L. H. Blumenschein, L. T. Gan, J. A. Fan, A. M. Okamura, and E. W. Hawkes, "A tip-extending soft robot enables reconfigurable and deployable antennas," *IEEE Robotics and Automation Letters*, vol. 3, no. 2, pp. 949–956, 2018.
- [20] F. Putzu, T. Abrar, J. Konstantinova, and K. Althoefer, "Eversion-type soft overtube for minimally invasive surgery," in *Hamlyn Symposium on Medical Robotics 2019*, 2019, pp. 7–8.
- [21] H. Godaba, F. Putzu, T. Abrar, J. Konstantinova, and K. Althoefer, "Payload capabilities and operational limits of eversion robots," in *Towards Autonomous Robotic Systems*, K. Althoefer, J. Konstantinova, and K. Zhang, Eds. Cham: Springer International Publishing, 2019, pp. 383–394.
- [22] T. Abrar, A. Hassan, F. Putzu, H. Godaba, A. Ataka, and K. Althoefer, "An inhomogeneous structured eversion actuator," in *Towards Autonomous Robotic Systems*, A. Mohammad, X. Dong, and M. Russo, Eds. Cham: Springer International Publishing, 2020, pp. 37–48.
- [23] F. Putzu, T. Abrar, and K. Althoefer, "Plant-inspired soft pneumatic eversion robot," in *2018 7th IEEE International Conference on Biomedical Robotics and Biomechanics (Biorob)*, 2018, pp. 1327–1332.
- [24] T. Abrar, F. Putzu, J. Konstantinova, and K. Althoefer, "Epm: Eversive pneumatic artificial muscle," in *2019 2nd IEEE International Conference on Soft Robotics (RoboSoft)*, 2019, pp. 19–24.